Electronic Supporting Information of

One-pot synthesis of iron-doped ceria catalysts for tandem carbon dioxide hydrogenation

Albert Gili, Maged Bekheet, Franziska Thimm, Benjamin Bischoff, Michael Geske, Martin Konrad, Sebastian Prätz, Christopher Schlesiger, Sören Selve, Aleksander Gurlo, Frank Rosowski, Reinhard Schomäcker

This supporting information contains figures S1 to S14, and tables S1 to S3.

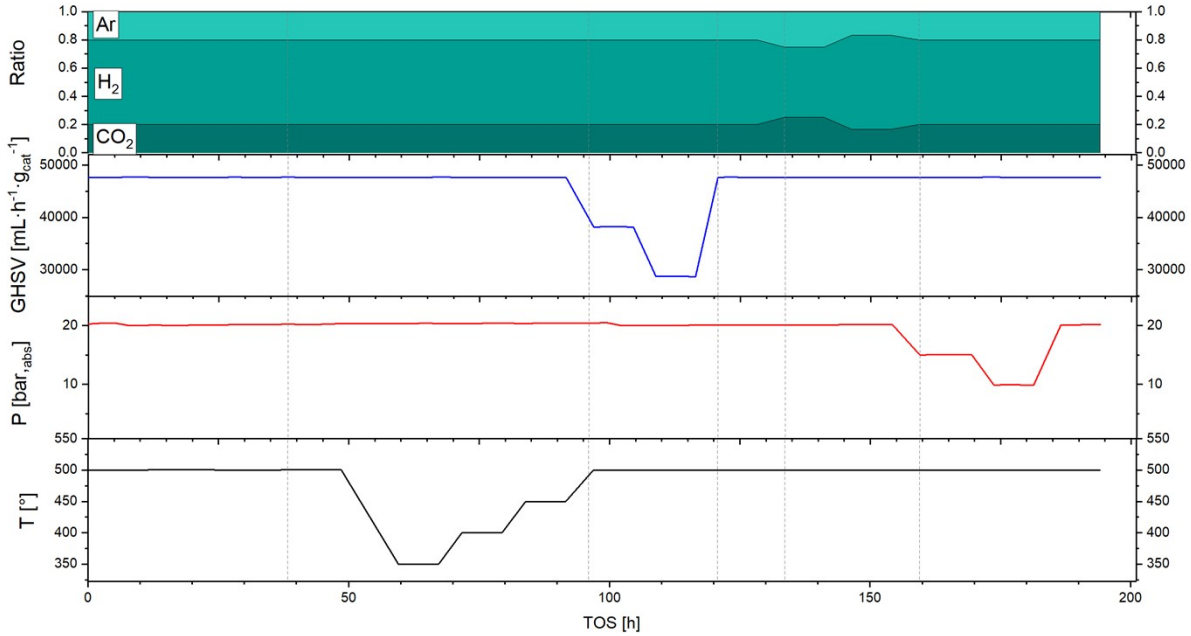

Figure S1. Graph with reactant ratio, GHSV, P and T as function of the TOS. The sensor real values for only reactor 1 are displayed to simplify visualization. Reactors 2 to 4 are not displayed but each data point (for the same conditions in between reactors) is approx. 30 min away from each other due to the GC analysis time.

Table S1. Full test conditions table. ~50 mg catalyst is loaded in each reactor. These include an initial reduction step (0) followed by an activation step/reference step (1), temperature variation (2-4), GHSV variation (5-6), reference (7), gas ratio variation (8-9), pressure variation (10-11), and a final reference step (12). All the reference steps are performed at the same operating conditions and allow assessing the performance stability.

Step		**GSHV**	**X_{H2}**	**X_{CO2}**	**X_{N2}**	**T**	**P**
		$mL \cdot h^{-1} \cdot g_{cat}^{-1}$	**%**	**%**	**%**	**ºC**	**Bar, (abs)**
0	Reduction	40000	10	0	90	500	20
1	Ref.	50000	60	20	20	500	20
2		50000	60	20	20	350	20
3	Temp.	50000	60	20	20	400	20
4		50000	60	20	20	450	20
5	GHSV	40000	60	20	20	500	20
6		30000	60	20	20	500	20
7	Ref.	50000	60	20	20	500	20
8	Ratio	50000	50	25	25	500	20
9		50000	67	17	17	500	20
10	Pressure	50000	60	20	20	500	15
11		50000	60	20	20	500	10
12	Ref.	50000	60	20	20	500	20

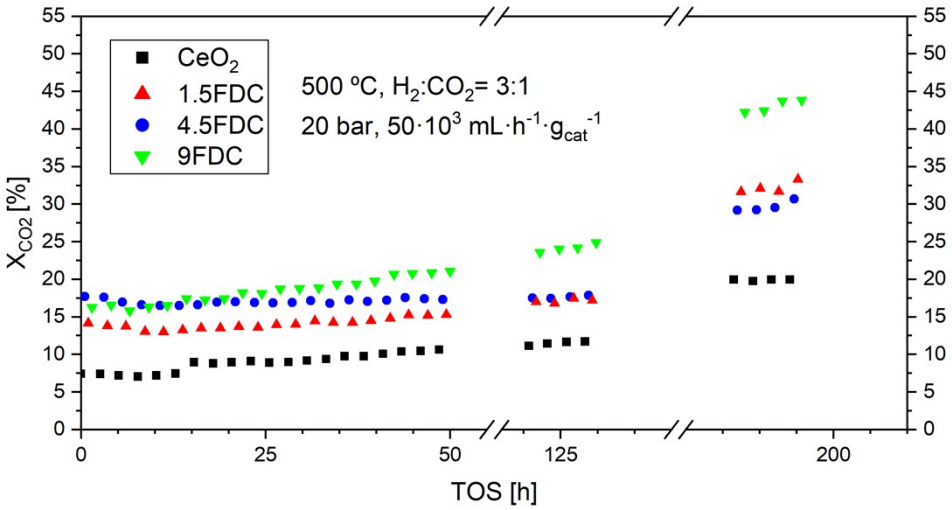

Figure S2. Conversion of CO_2 with TOS for all the catalysts. The conditions are: 500 °C, H_2:CO_2:Ar=3:1:1, 20 bar and 50,000 mL·h^{-1}·g_{cat}^{-1}. Although not strictly a stability test, this experiment shows the change in the conversion of CO_2 over the full tested period.

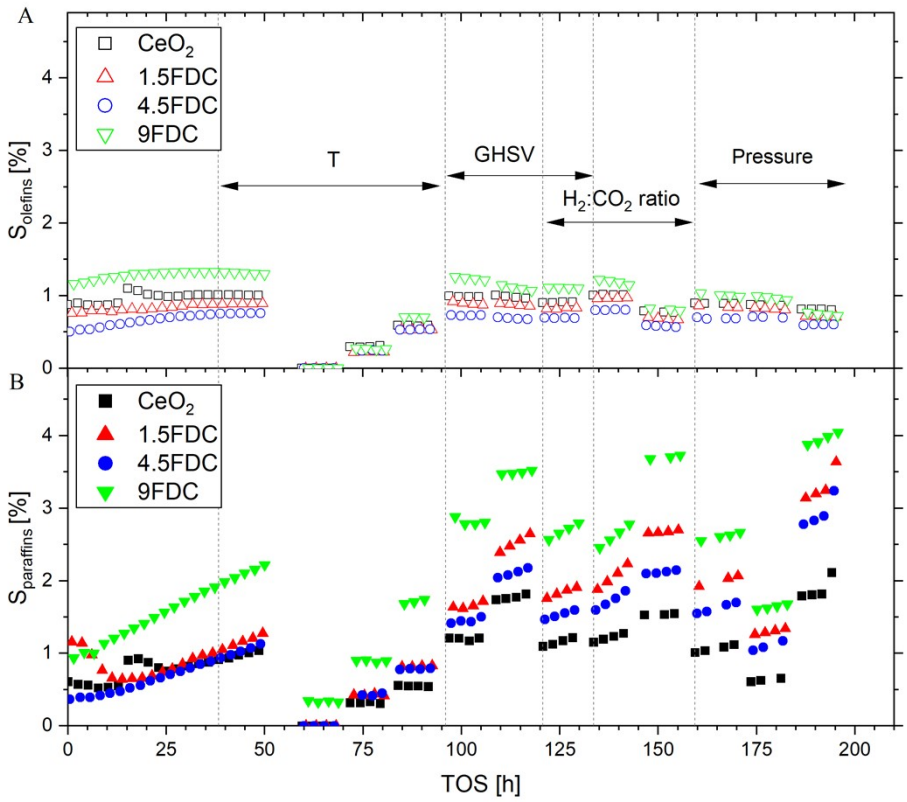

Figure S3. Selectivity toward C2-C4 olefins (top panel) and paraffins (bottom panel) for all samples as function of TOS.

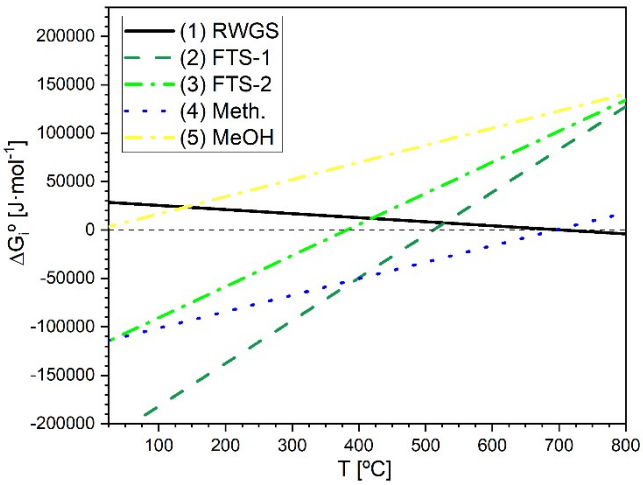

Figure S4. Gibbs free energy as function of the temperature for reactions 1-5. Reaction 1-RWGS, $CO_2 + H_2 \leftrightarrow H_2O + CO$*; Reaction 2-FTS-1,* $5H_2 + 2CO \leftrightarrow C_2H_6 + 2H_2O$*; Reaction 3-FTS-2,* $4H_2 + 2CO \leftrightarrow C_2H_4 + 2H_2O$*; Reaction 4-Meth,* $4H_2 + CO_2 \leftrightarrow CH_4 + 2H_2O$*; Reaction 5-MeOH,* $3H_2 + CO_2 \leftrightarrow CH_3OH + H_2O$

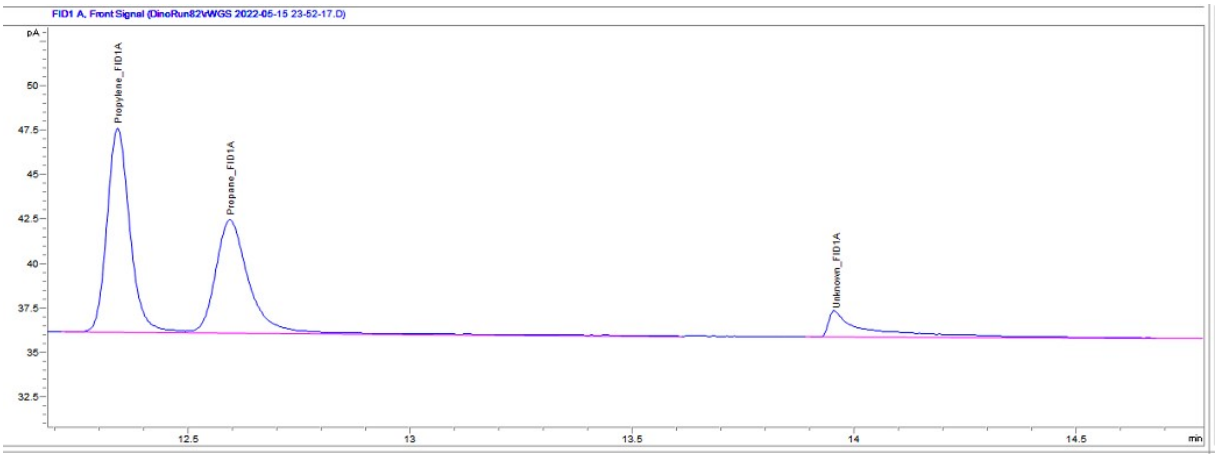

Figure S5. Unidentified peak detected during GC analysis. The quantified species in the GC were carbon dioxide, carbon monoxide, hydrogen, nitrogen, argon, methane, ethane, propane, n-butane, n-pentane, n-hexane, n-heptane, ethylene, propylene, n-butane, methanol, ethanol, n-propanol, n-butanol, dimethyl ether, acetaldehyde, propanal, butanal, formic acid, acetic acid, Methylformate, methylacetate, and ethylacetate.

Table S2. Iron concentration obtained with ICP-OES, wt.% of S obtained with the combustion method, and specific surface area obtained with N_2-adsorption BET for all the fresh samples.

Sample	**Fe mol%**	**S wt.%**	**SSA [$m^2 \cdot g^{-1}$]**
CeO_2	0.042	0.020	4.5
1.5FDC	1.36	0.019	14.7
4.5FDC	4.20	0.024	14.1
9FDC	8.77	0.020	10.6

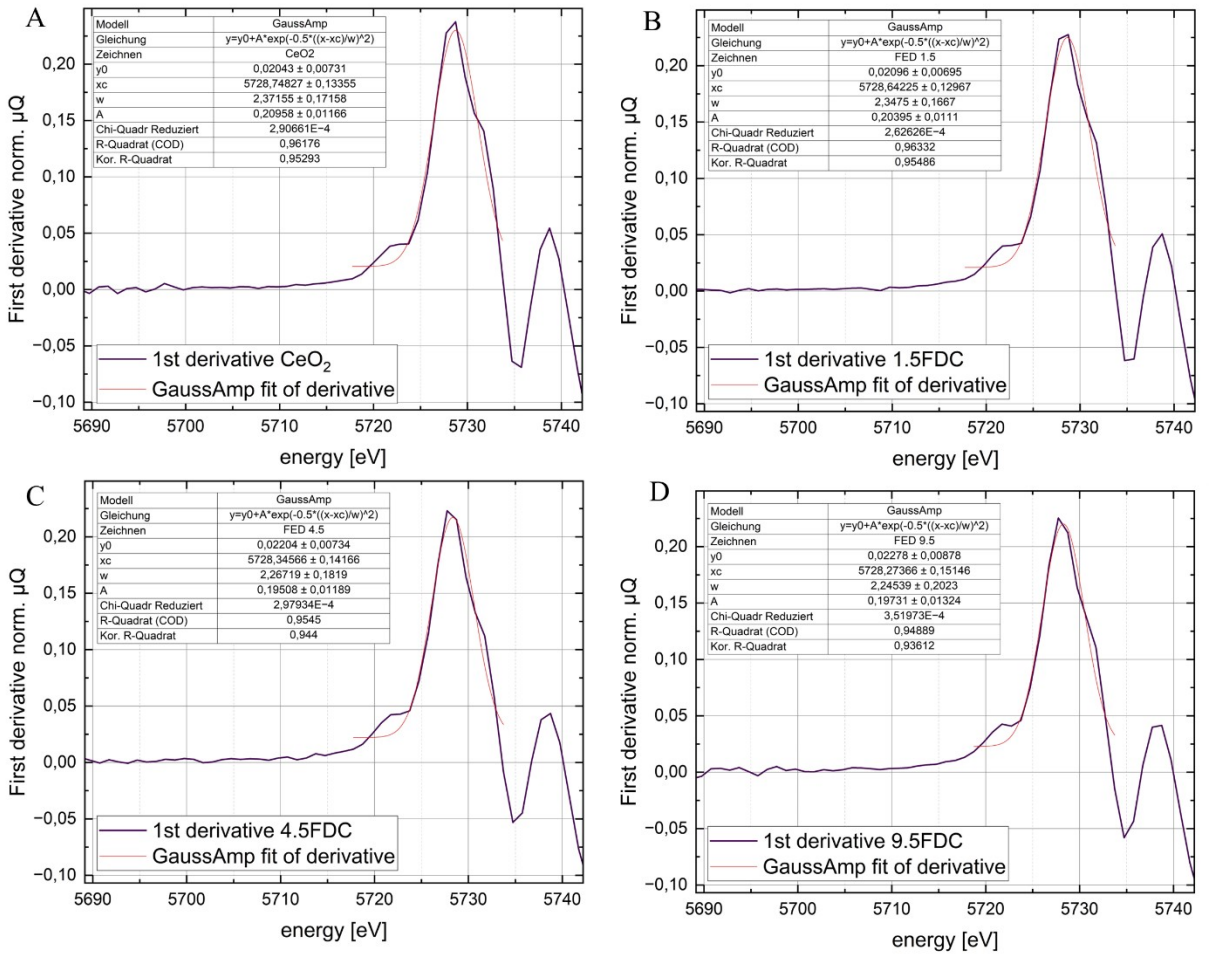

Figure S6. Fitting results of the Ce L_3 X-ray absorption data shown in figure 3 of the manuscript. The 1st derivate of the edge was fitted using a Gaussian function. The specified uncertainty of the edge positions is the std. of the gaussian fits. The 1st derivative was fitted with a Gaussian fit in the energy range of 5716 to 5734 by using Origin2020

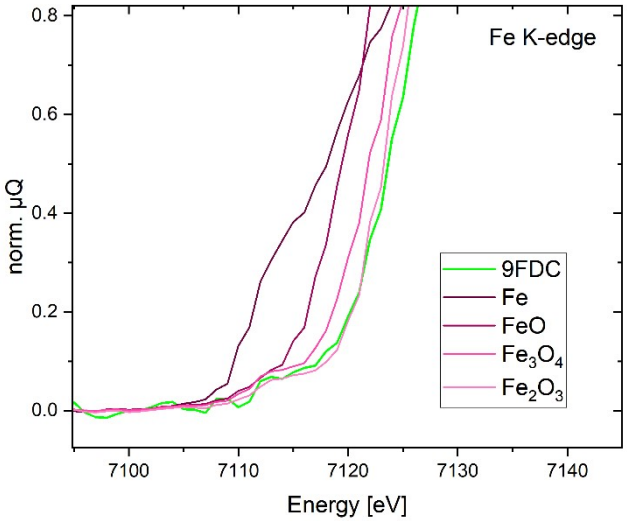

Figure S7. Pre-edge XANES spectra of the Fe K-edge of the 9FDC sample and the reference materials. The best match clearly occurs with the Fe^{3+} reference material.

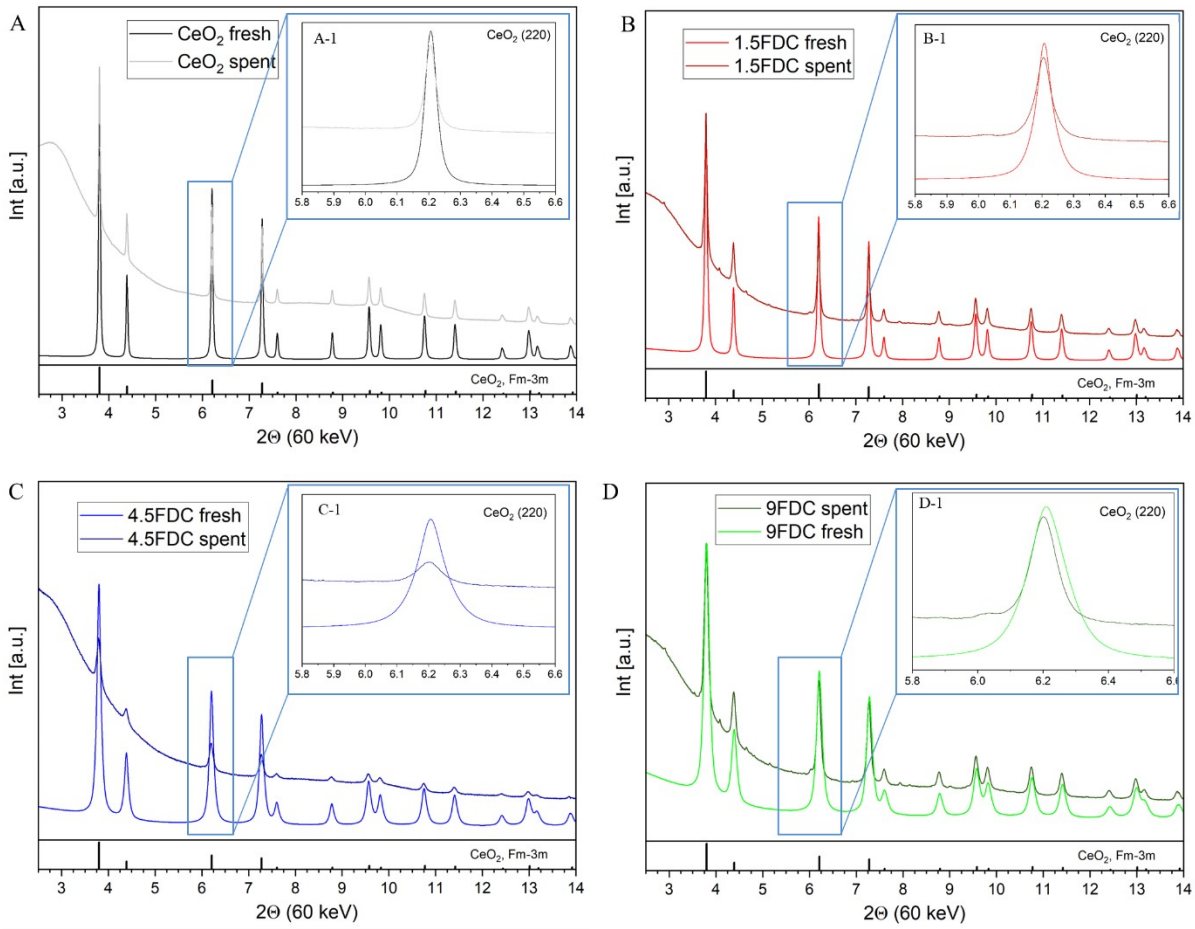

Figure S8. XRD data of the fresh and spent samples with (insight) magnification of the CeO_2(220) reflection. All the data has been normalized. The spent 4.5FDC sample yielded particularly low counts due to few present catalyst grains in the analyzed sample. All data was acquired at 60 keV and with time expositions between 60 and 180 s.

Table S3. Rietveld refinement of the XRD data.

Sample	Space group	Fresh sample		Spent sample	
		Lattice parameter [Å]	Crystallite size [nm]	Lattice parameter [Å]	Crystallite size [nm]
CeO_2	*Fm-3m*	5.4115(2)	23.6	5.4130(2)	31.6
1.5FDC	*Fm-3m*	5.4106(2)	13.7	5.4135(2)	15.1
4.5FDC	*Fm-3m*	5.4101(2)	7.5	5.4162(2)	10.0
9FDC	*Fm-3m*	5.4067(2)	5.8	5.4155(2)	9.5

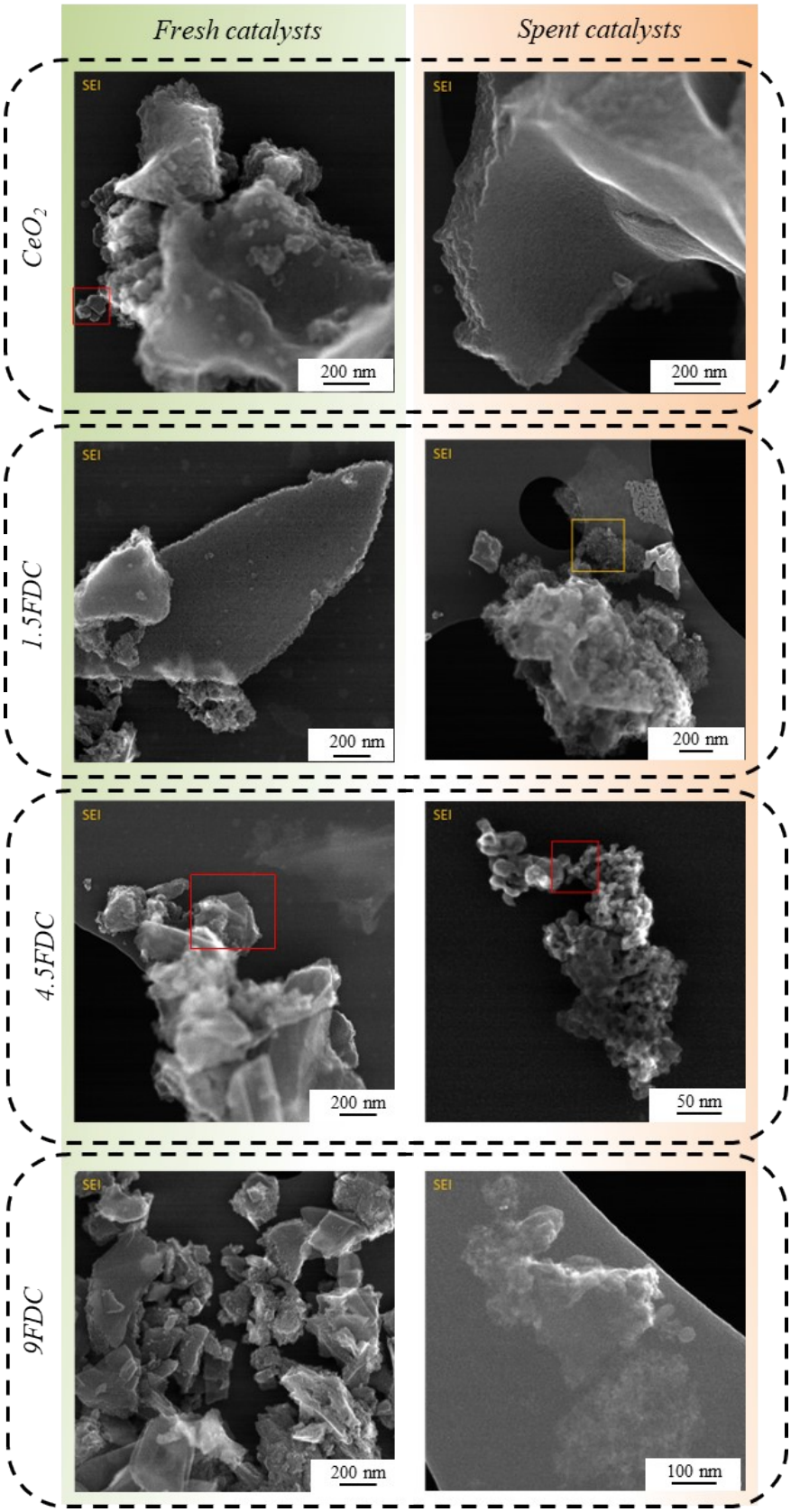

Figure S9. STEM images of the samples at lower magnification. If present, the colored frames highlight the regions displayed in the figure 5 of the main manuscript.

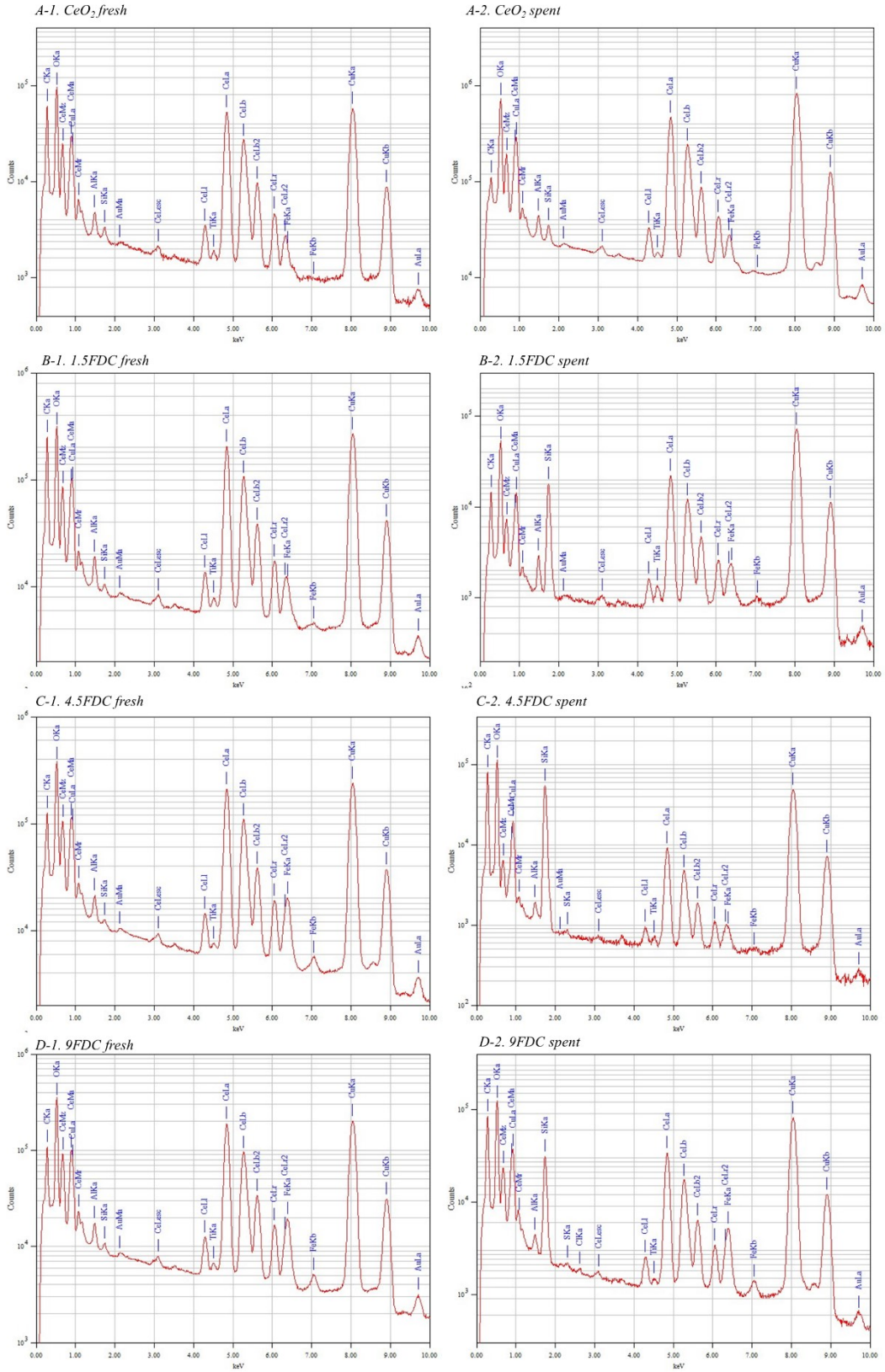

Figure S10. EDX spectra of all the fresh and spent samples shown in figure 5 of the manuscript.

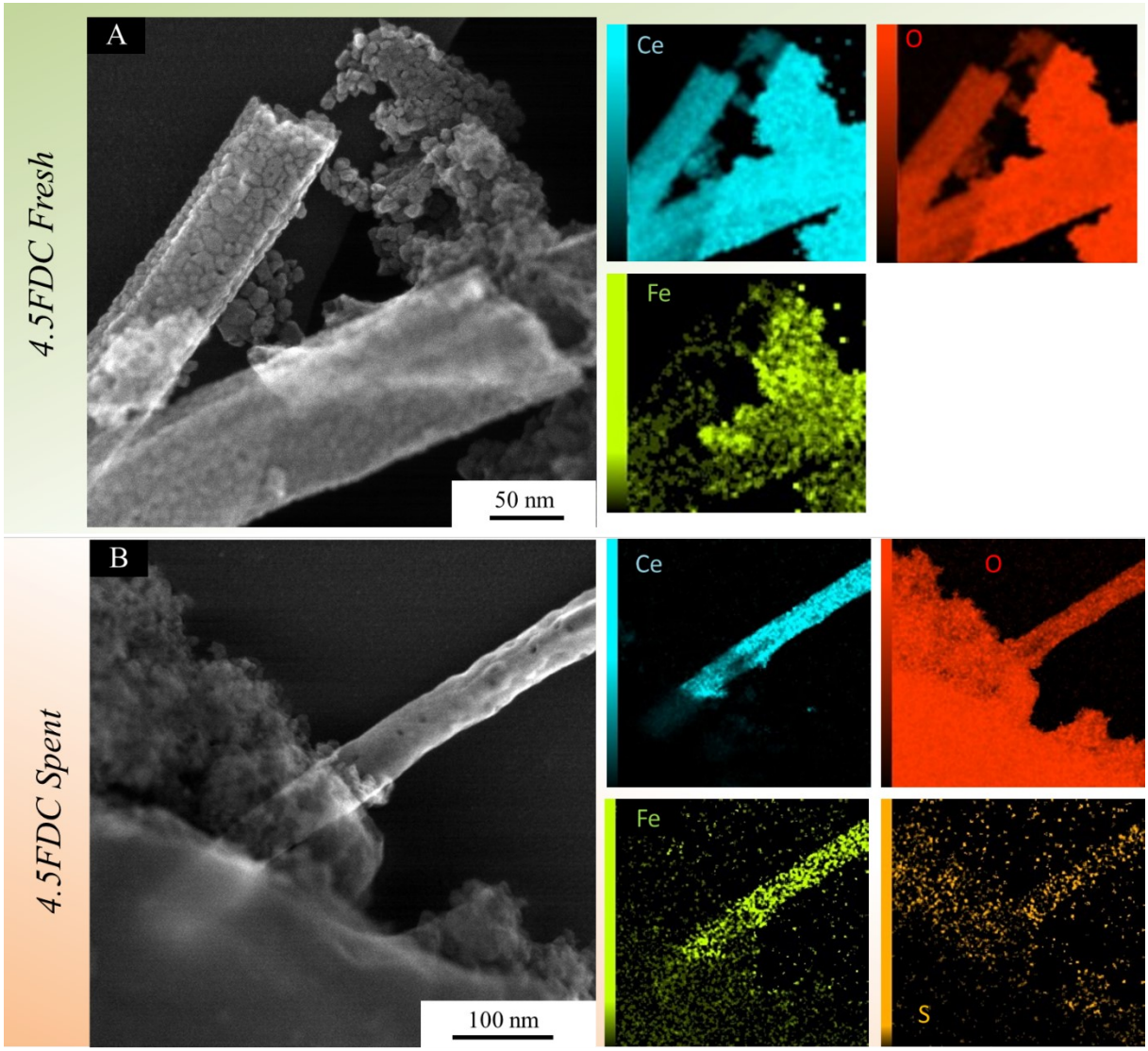

Figure S11. 4.5FDC STEM. No S was detected in the fresh sample, whereas 0.9 wt.% S was detected in the spent catalyst.

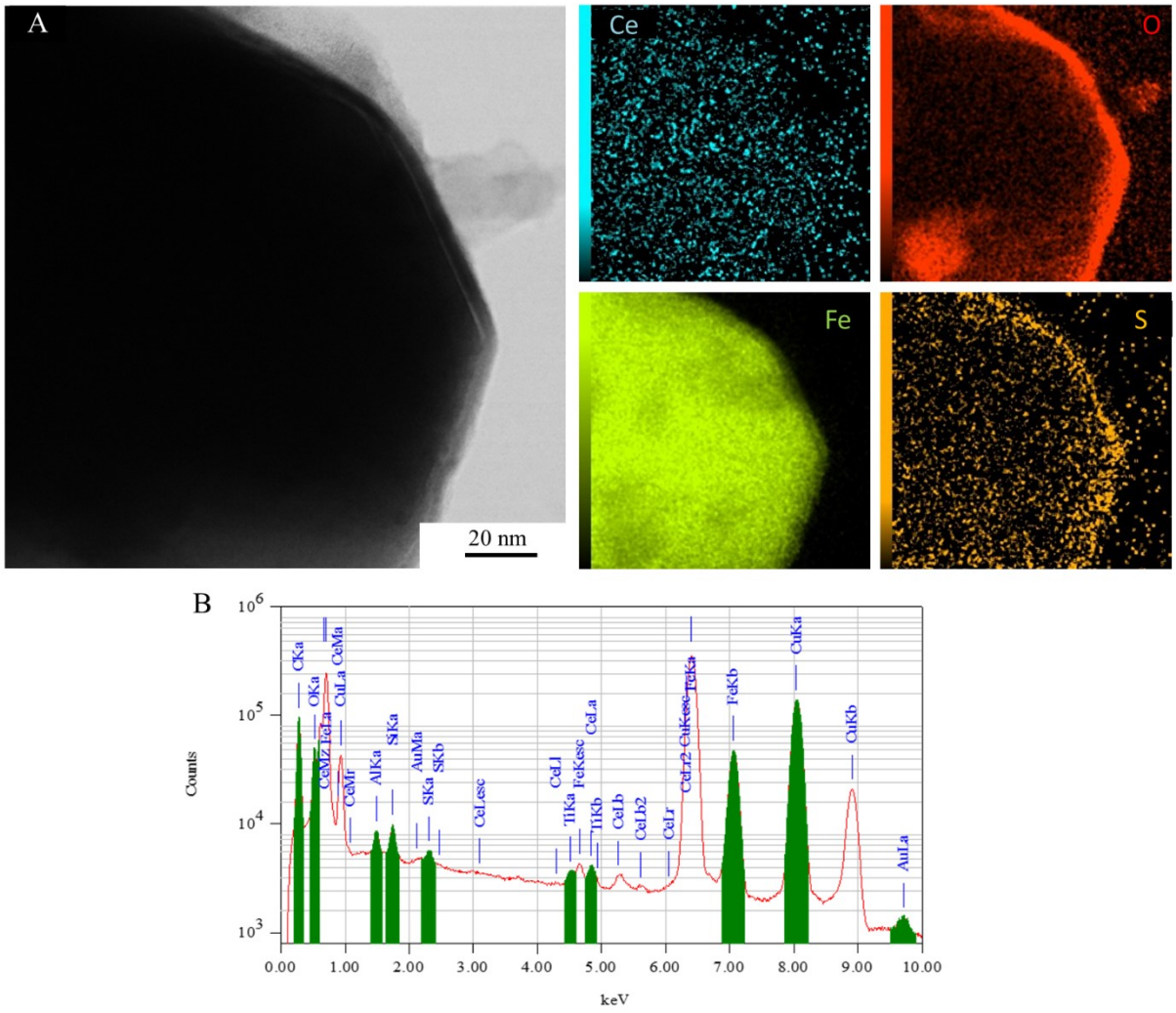

Figure S12. STEM-BF of the spent 4.5FDC showing an exsoluted particle. The same type of structure as for the 9FDC sample described in the main manuscript is observed. In this case, a S-content of 0.14 wt.% and Ce of 0.89 wt.% are quantified. EDX spectra (panel B) and mapping.

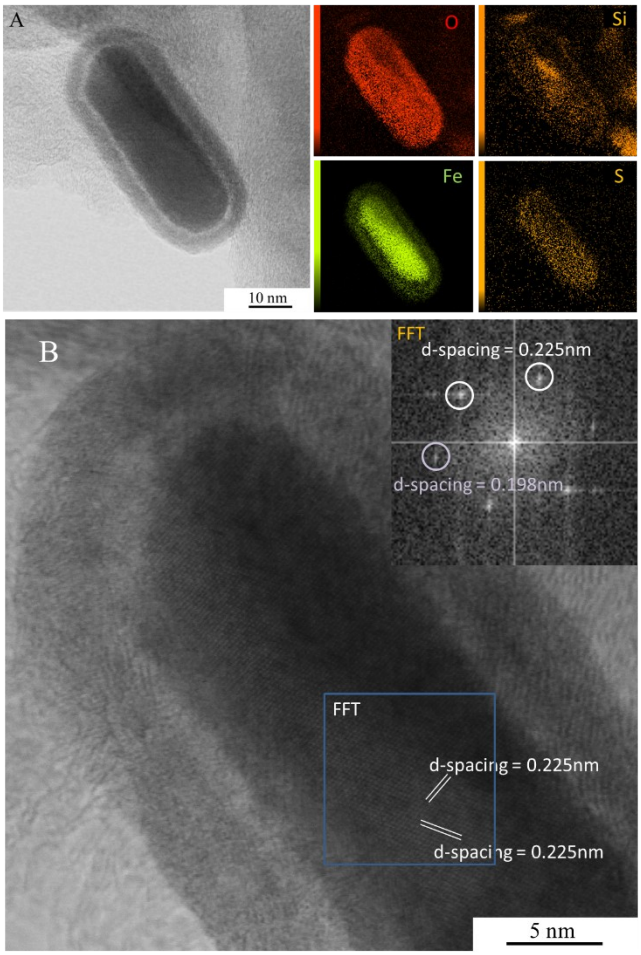

Figure S13. HR-STEM-BF of the spent 9FDC. Panel A: view of the core-shell particle and EDX elemental mapping. The quantitative analysis yields contents of 32.62 %wt. (O), 3.17 %wt. (Si), 0.73 %wt. (S) and 63.47 %wt. (Fe). Panel B: FFT of the core of the particle showing d-spacings of 0.225 nm and 0.198 nm. The angles between both 0.225 nm reflections is measured to 68.6° and between 0.225 nm and 0.198 nm is measured to 53.6° (resp. 57.6° for the opposite reflection).

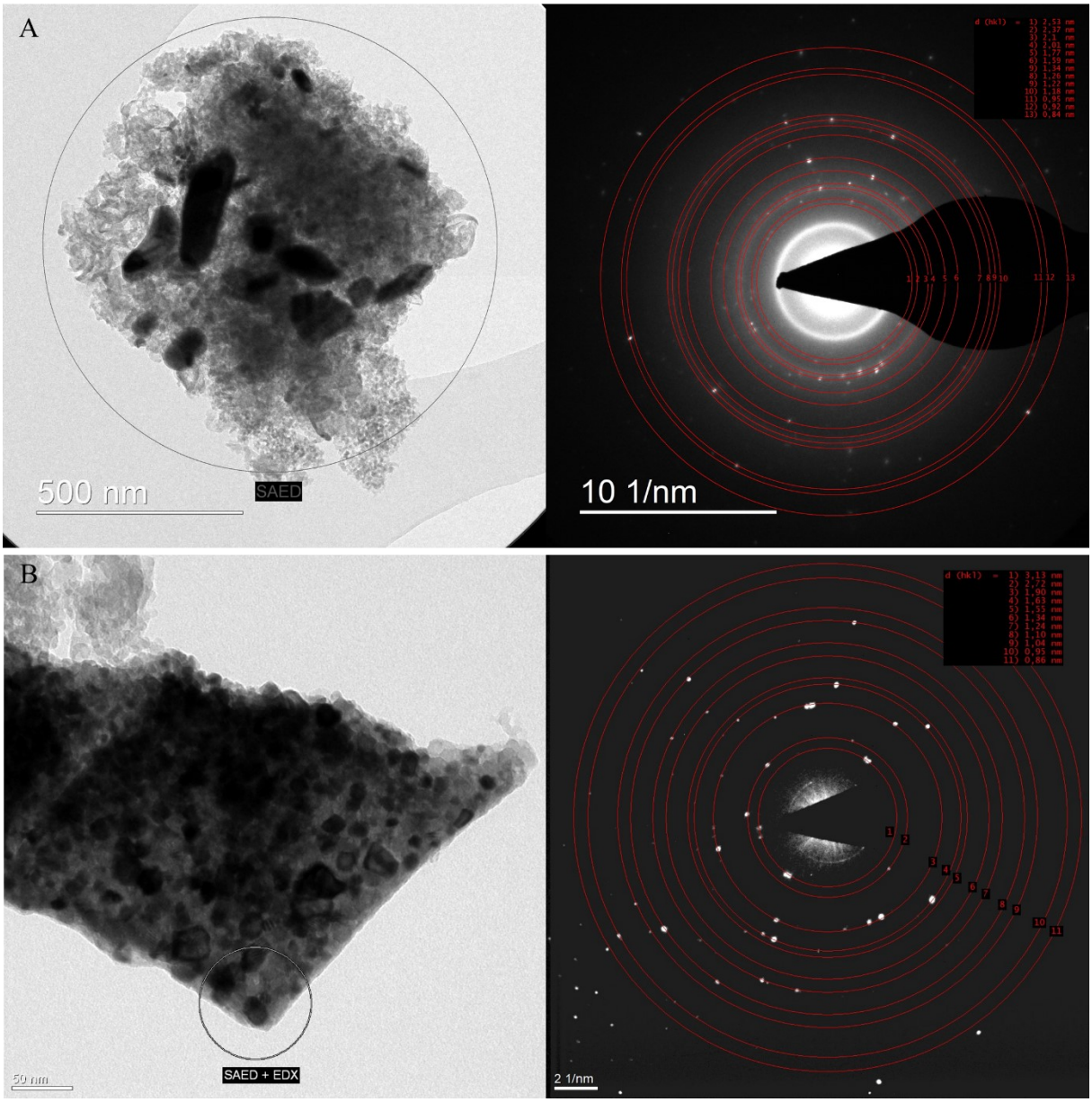

Figure S14. TEM imaging of the 9FDC spent catalyst (left column) with SAED (right column) of the areas highlighted. Panel A allows to identify the interplanar distances of Fe_3C (*Pnma*, PDF 00-035-0772) phase, whereas Panel B reflections fit the CeO_2 (*Fm-3m*, 00-034-0394) phase.